Supplementary Materials & Methods

Drosophila strains & genetics

UAS-cg flies were made by amplifying the coding region from BDGP DGC cDNA clone LD05357 with oligos 5'- CATGGTACCTGTGCCGCCCAGAATCCGCC-3' and 5'-CACTCTAGACTAGCATACCTGTTGCTGCGATATGGCTG-3', subcloning into pUASt-FLAG-attB and integrating into the ϕC31 86FB landing site (Bischof et al., 2007).

The *RNAi* transgenes targeting *cg* are predicted to degrade hundreds of off-target transcripts and produced phenotypes we never observed in *cg* mutants (data not shown), while the perdurance of maternally deposited Cg protein (Ray et al., 2016) masked the null phenotype in all but the earliest-generated mitotic clones. We bypassed these problems by hand-picking first instar homozygous *cg* mutant larvae. These animals normally die at early larval stages when faced with competition from their heterozygous siblings, but when isolated and cultured independently, a small fraction survive to the late third instar, enabling analysis of their eye-antennal discs.

To determine the roles of *eya* and *so* and to assess their interactions with other genes in the SMW, we crossed *GMR-GAL4^{Zipursky}/CyO,act-GFP* or *GMR-GAL4^{Zipursky},UAS-eya^{RNAi}/CyO,dfd-YFP* to *w^{1118}*, *UAS-so^{RNAi}*, *UAS-stg^{RNAi}*, *pnt$^{\Delta 88}$/TM3,Ser,twi-GAL4,UAS-GFP*, *ttk^{1e11}/TM6B,Hu,Tb*, *FRT42D,cg^{A22}/CyO,dfd-YFP*, or *UAS-cg*. Genetic interactions between *eya* and *cg* were assessed by crossing *ey-GAL4*, *ey-GAL4,UAS-eya^{RNAi}*, *GMR-GAL4^{Zipursky}/CyO,act-GFP*, or *GMR-GAL4^{Zipursky},UAS-eya^{RNAi}/CyO,dfd-YFP* to *w^{1118}*, *FRT42D,cg^{A22}/CyO,dfd-YFP*, or *Df(2R)BSC401/CyO*. For ectopic Dac induction experiments, we crossed *dpp^{40C6}-GAL4/TM6B,Hu,Tb*, *dpp^{40C6}-GAL4,UAS-eya^{IIIa}/TM6B,Hu,Tb*, *dpp^{57A1}-GAL4/CyO,dfd-YFP*, or *dpp^{57A1}-GAL4,UAS-eya^{1}/CyO,dfd-YFP* to *w^{1118}*, *FRT42D,cg^{A22}/CyO,dfd-YFP*, or *UAS-cg*. To determine the role of *cg* in the eye-antennal imaginal disc, including the SMW, and to assess its genetic interaction with *eya* and *so*, we crossed *FRT42D,cg^{A22}/CyO,dfd-YFP* to *eya^{Clift},FRT42D,cg^{A22}/CyO,dfd-YFP* or *FRT42D,so^{3},cg^{A22}/CyO,dfd-YFP* and compared with *w^{1118}*. Mitotic or whole-eye clones were made by crossing *ey-FLP;FRT42D,ubi-GFP/CyO* or

y^1,w^*;FRT42D,y^+,GMR-hid,l(2)CL-R^1/Cyo;ey-GAL4,UAS-FLP to *FRT42D*, *FRT42D,cg^{A22}/CyO,dfd-YFP*, *eya^{Clift},FRT42D,cg^{A22}/CyO,dfd-YFP*, or *eya^{A188},FRT42D,cg^{A22}/CyO,dfd-YFP*. Flies were reared on standard cornmeal-molasses-agar medium and all crosses were at 25°C.

Immunohistochemistry & Microscopy

Primary antibodies: rabbit α-PH3 (1:2000, Upstate, 06-570), rat α-ELAV (1:50, Developmental Studies Hybridoma Bank [DSHB], 7E8A10) (O'Neill et al., 1994), guinea pig α-Eya (1:1000) (Silver et al., 2003), mouse α-Dac (1:10, DSHB, mAbdac2-3) (Mardon et al., 1994), rabbit α-FLAG (1:500, Sigma, F1804), mouse α-Delta (1:1000, DSHB, C594.9B) (Fehon et al., 1990), mouse α-Cut (1:100, DSHB, 2B10) (Blochlinger et al., 1990), rabbit α-cleaved caspase 3 (1:1000, Cell Signaling), and mouse α-Pros (1:100, DSHB, MR1A) (Campbell et al., 1994). Secondary antibodies were from Jackson ImmunoResearch: donkey α-rabbit-Cy3 (1:2000), donkey α-rabbit-488 (1:2000), donkey α-rat-Cy3 (1:2000), donkey α-rat-488 (1:2000), donkey α-mouse-Cy3 (1:2000), or donkey α-guinea pig-488 (1:2000). Oregon Green 488 Phalloidin (1:2000, Thermo Fisher Scientific) and DAPI (1:2000, Invitrogen) were used to detect actin and DNA, respectively. The Click-iT EdU Alexa Fluor 594 Imaging Kit (Molecular Probes, C10339) was used to label DNA synthesis.

For antibody staining, third instar eye-antennal imaginal discs were dissected in S2 cell medium, fixed for 10 min in 4% paraformaldehyde with 0.1% Triton X-100, washed 3X in PBT (1X PBS, 0.1% Triton), blocked in PNT (1X PBS, 0.1% Triton, 1% normal goat serum), stained with primary antibodies in PNT overnight at 4° C, washed 3X in PBT, and stained with secondary antibodies in PNT for 2 h at room temperature or overnight at 4° C. Pupal and adult tissues were treated in the same manner, except that halved heads were fixed for 20 min prior to dissecting the retinas, and then post-fixed for 10 min.

For S-phase detection, dissected discs were incubated in 10 μM EdU in PBS for 60 min at room temperature, rinsed 5 min in PBS, fixed for 15 min in 4% paraformaldehyde in PBS, washed 3X 5 min in PBS with 0.3% Triton X-100 (PBT3), washed 20 min in PBS

with 0.6% Triton X-100 (PBT6), washed 2X 5 min in PBT3 with 3% BSA (PBT3B), incubated in the Click-iT reaction mixture 30 min in the dark, washed 5 min in PBT3B; washed 2X 5 min in PBT and mounted.

All primary antibodies used in this study are standard reagents in the fly eye field and have been subject to extensive prior validation. Additional validation of antibody specificity from our study included comparison of expression pattern, levels and subcellular localization in wild type versus mutant or overexpressed imaginal tissues and in transiently transfected S2 cells, as well as recapitulation of previously described and published expression patterns.

In vitro *pulldown assays*

GST-fusion proteins were expressed in BL21 *E. coli* cells, bound by Protino Glutathione Agarose 4B (Machery-Nagel), washed, and cleaved by TEV protease as necessary. Pulldown assays were performed by mixing equimolar amounts of the desired proteins in binding buffer (20 mM Tris, 100 mM NaCl, 0.1 mM EDTA, 2.5 mM $MgCl_2$, 0.1% NP-40, 10% glycerol, 100 ug/mL BSA). Binding reactions were incubated at 4° C for 2 h in the presence of glutathione sepharose resin, washed 3X in binding buffer with either 100 mM, 500 mM, or 1 M NaCl, boiled, resolved by SDS-PAGE, immunoblotted and imaged on a Li-COR Odyssey.

Transcription Assays in cultured S2 cells

2.25 x 10^6 of *Drosophila* S2 cells plated in 12-well plates in 1.5 mL of Schneider's medium (Sigma) with 10% insect medium supplement (Sigma), penicillin (Invitrogen), and streptomycin (Invitrogen) were transfected in duplicate with a mixture of dimethyl-dioctadecyl-ammonium bromide (DDAB) (Sigma) containing 750 ng of total plasmid DNA. After 48 h, cells were lysed in 100 mM KH_2PO_4, 0.5% NP-40, and 1 mM DTT at pH 7.8, incubated 1 h on ice, spun, and loaded into a tube luminometer in triplicate 50 µL aliquots (EG&G Berthold Autolumat LB953). Firefly and Renilla luciferases were activated by exposure of lysates to 100 µL of 0.01 M Magnesium acetate, 0.1 M Tris acetate, 1 mM EDTA, 76.9 µM luciferin (BD Pharmingen), and 4.62 mM ATP (Fisher) at pH 7.8 or 25 mM Sodium pyrophosphate, 10 mM Sodium acetate, 15 mM EDTA, 0.5 M

Na_2SO_4, 0.5 M NaCl, and 4 μM coelenterazine (Promega) at pH 5.0, respectively. Empty vector was used to standardize the amount of DNA transfected across conditions, and all measurements were normalized to the activity of Renilla luciferase expressed under the control of an *actin* promoter.

To generate the 2X-LMEE reporter, we inserted a SalI restriction site into the multiple cloning site of pBS-TATA-luciferase (Silver et al. 2003) and ligated in two copies of the *LMEE* sequence amplified with 5'-CAGCTCGAGAGCGCACATTCTTGCCACATCCTTG-3' and 5'-GCGGTCGACCATTAACAAAATAAAAAAGGGGAACGACTCGTGCG-3'. The Gateway system (Invitrogen) was used to insert the full-length *cg* cDNA, amplified with 5'-CGCGGATCCGGCTGTGCCGCCCAGAATCCG-3' and 5'-TGGCTCGAGAGTCTAGCATACCTGTTGCTGCGA-3' and subcloned into pENTR-3C, into the actin5C S2 cell expression vector pAFW.

S2 cells were replaced from frozen stocks every six months and were not authenticated or tested for contamination within that interval.

Supplementary Figures

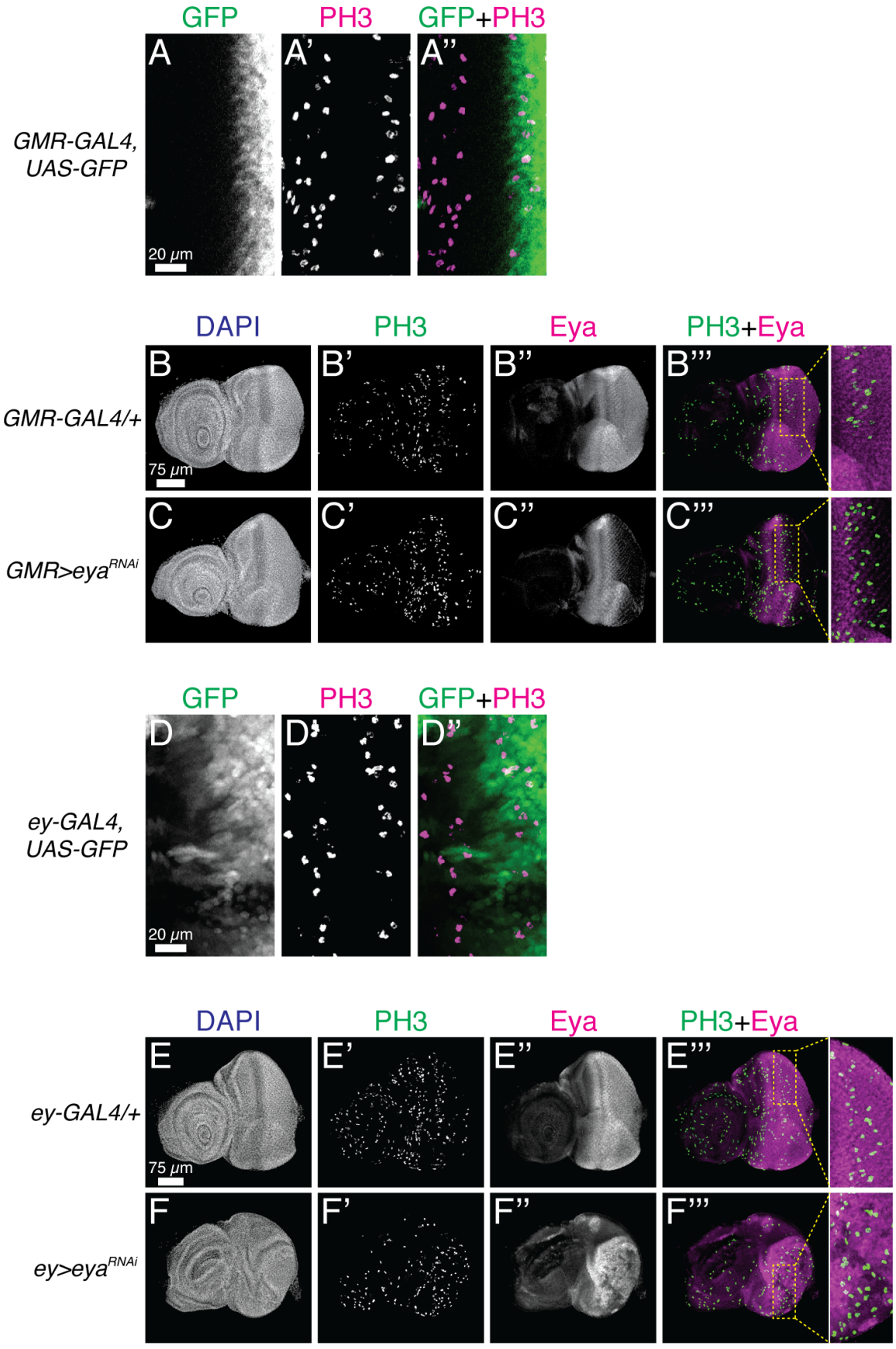

Fig. S1. Knockdown under *GMR-GAL4* depletes protein levels by the SMW. All images are maximum projections through representative third instar eye-antennal imaginal discs. Anterior is to the left and dorsal is up. PH3 was used to mark the SMW (A) *GMR-GAL4* drives GFP expressio in a domain overlapping the SMW. Panels are zoomed views centered on the MF. (B-C) *eya* knockdown under *GMR-GAL4* strongly reduces Eya protein levels at the SMW. (D) *ey-GAL4* drives GFP expression at and before the SMW. (E) *eya* knockdown under *ey-GAL4* lowers Eya protein levels before and in the SMW and increases SMW proliferation posterior to the MF.

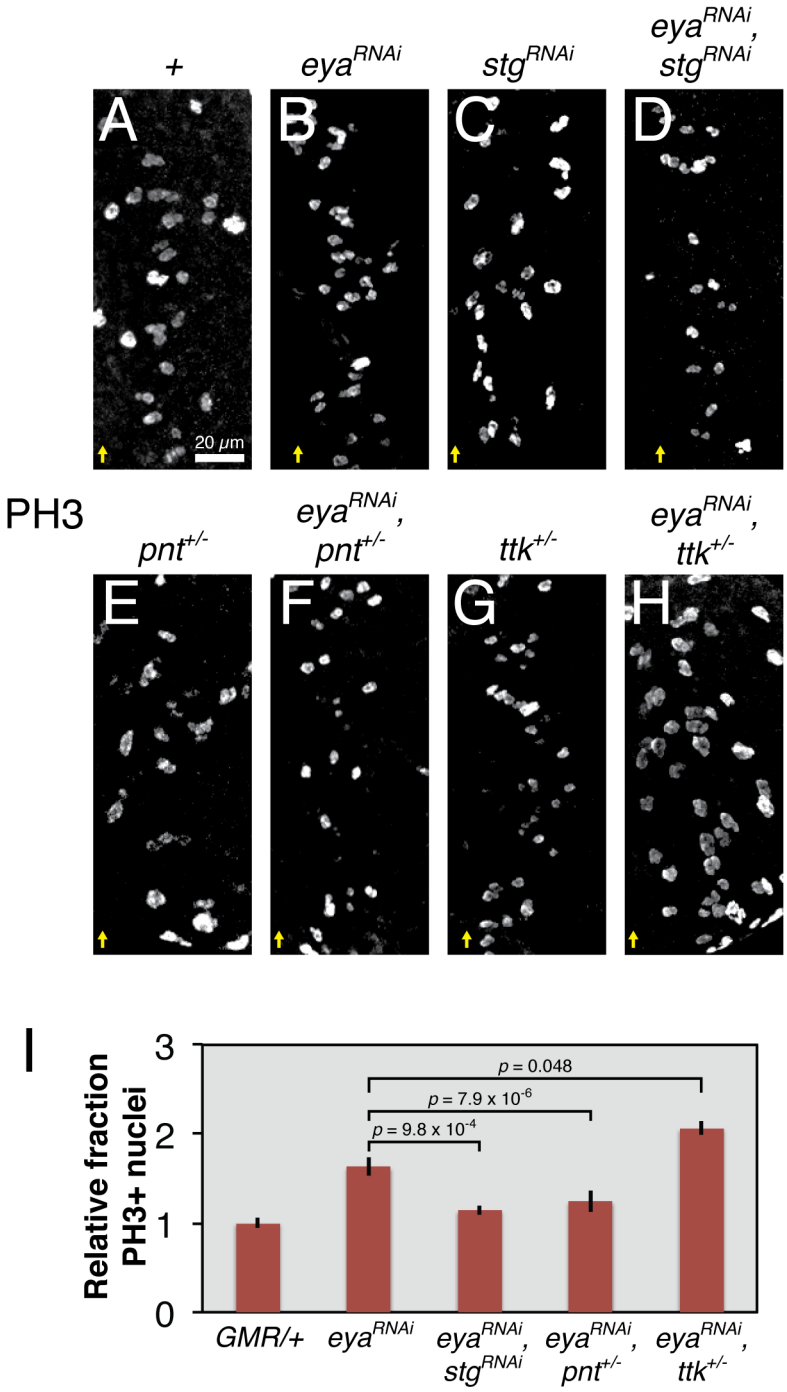

Fig. S2. Genetic interactions between *eya* and M phase regulators at the SMW. All images show representative late third instar eye-antennal imaginal discs. Yellow arrows mark the ventral edge of the MF. *UAS* transgenes were expressed with *GMR-GAL4*. (A-D) Dominant suppression of the increased SMW mitotic rate in *eya* knockdown discs by weak *string* knockdown that on its own does not impair the SMW. (T-W) Dominant suppression and enhancement of the *eya*

knockdown SMW phenotype by reducing the dose of *pnt* or *ttk*, respectively. (X) Quantification of mitotic rates for genotypes in P-W ($n \geq 7$), calculated as in G. Actual PH3 counts for C-F and P-W in Supplementary Table 1.

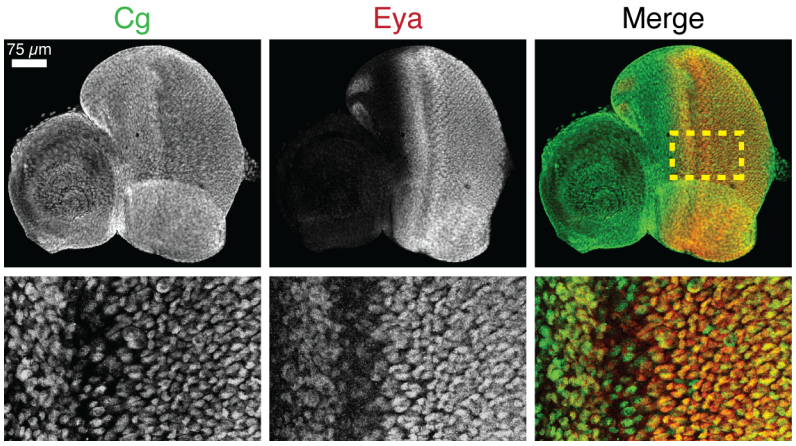

Fig. S3. Cg and Eya are co-expressed in the eye imaginal disc. A homozygous *cg-GFP* disc was stained with rabbit anti-GFP and guinea pig anti-Eya. The top row shows maximum confocal projections, while the zoomed views in the bottom row are partial projections focused on the photoreceptors. The yellow box shows the position of the zoomed panels in the disc.

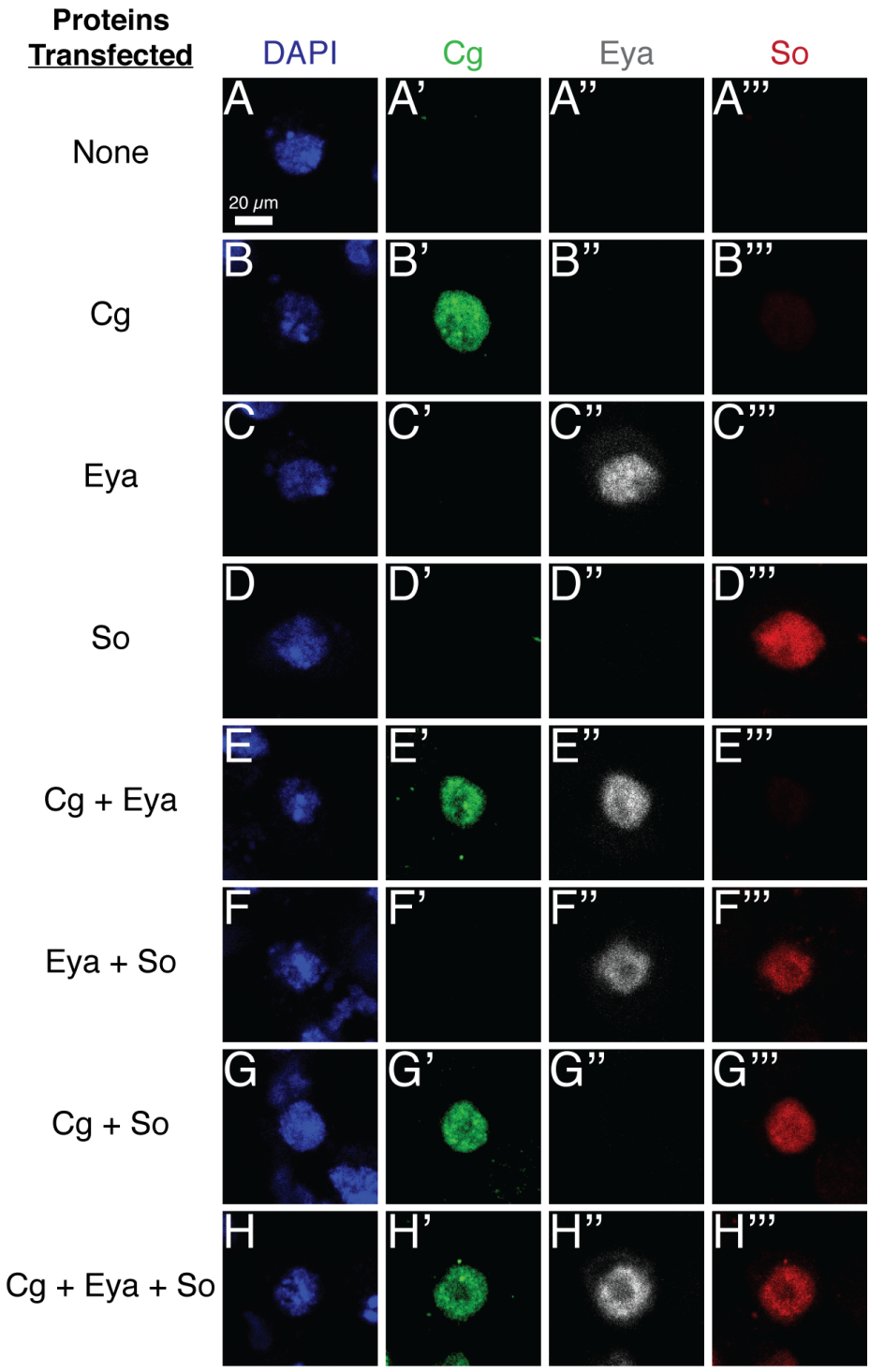

Fig. S4. Eya, So, and Cg co-localize in the nuclei of cultured S2 cells. All images are single confocal slices through the nuclei of representative S2 cells. Cells were transiently transfected with plasmids encoding the proteins indicated to the left of each row, fixed, and stained for the proteins indicated above each column.

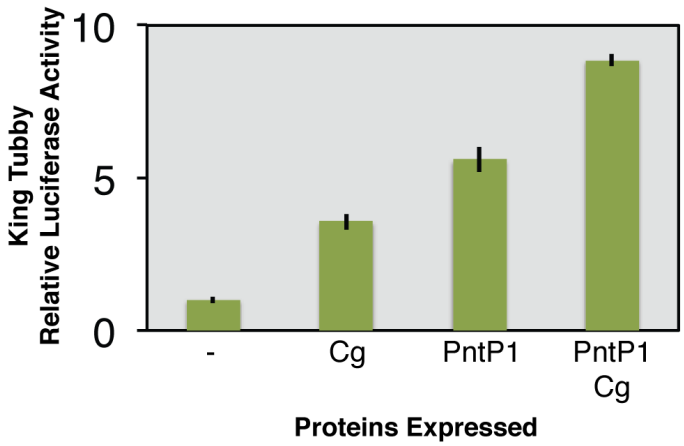

Fig. S5. Cg does not limit the ability of PntP1 to activate transcription. Experimental conditions are identical to Fig. 3A, except for expression of PntP1 and use of a Pnt-responsive *King Tubby* reporter (Webber et al., 2013). This experiment was replicated independently twice. Note that Cg alone activates expression of this reporter and additively increases output relative to PntP1 alone.

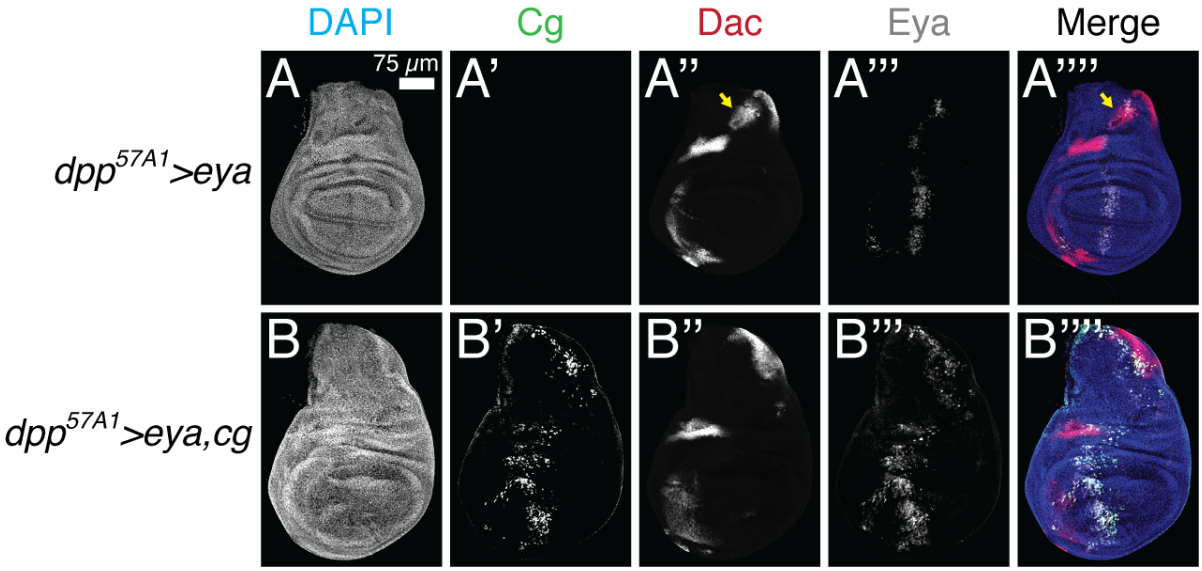

Fig. S6. Co-overexpressing *cg* does not reduce Eya levels in wing imaginal discs. Experimental and imaging conditions are identical to Fig. 3F and H, except that the tissue was also stained with guinea pig anti-Eya. The aberrant folding in discs co-overexpressing *eya* and *cg* expanded the Eya expression stripe, making the reduced induction of ectopic Dac even more striking.

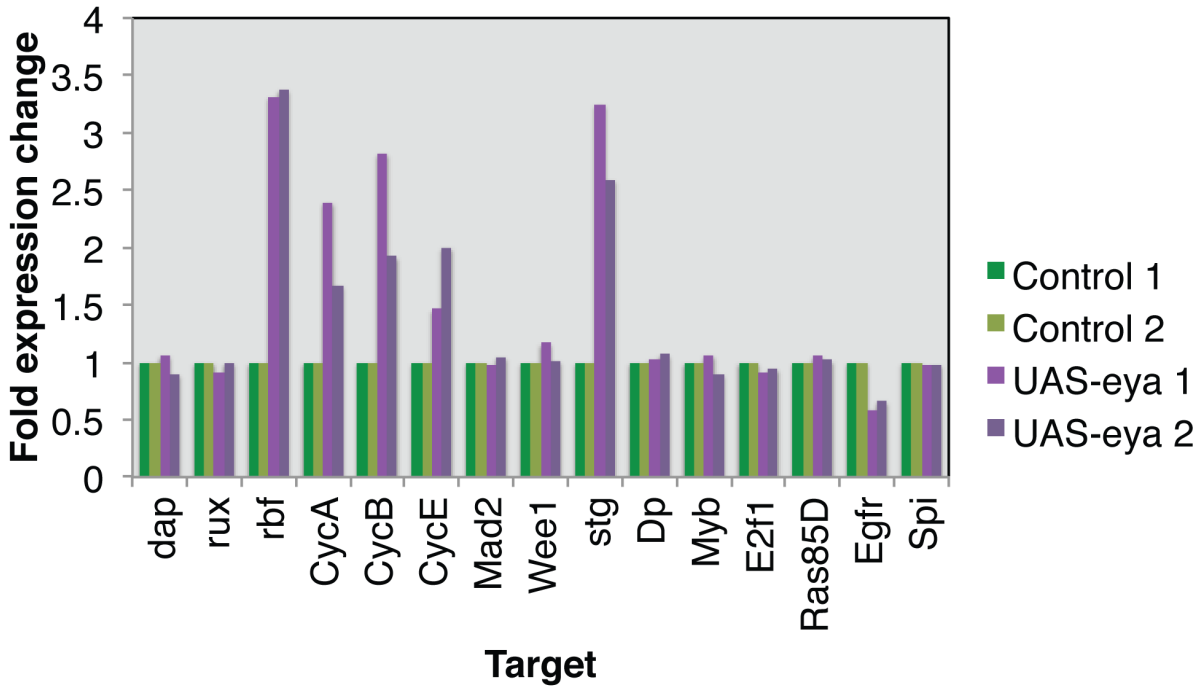

Fig. S7. The effect of *eya* overexpression on the transcription of cell cycle regulators in the eye-antennal imaginal disc. Raw data were obtained from Jemc et al., 2007. Two experimental replicates are shown. All bars are normalized to the control conducted with that replicate.

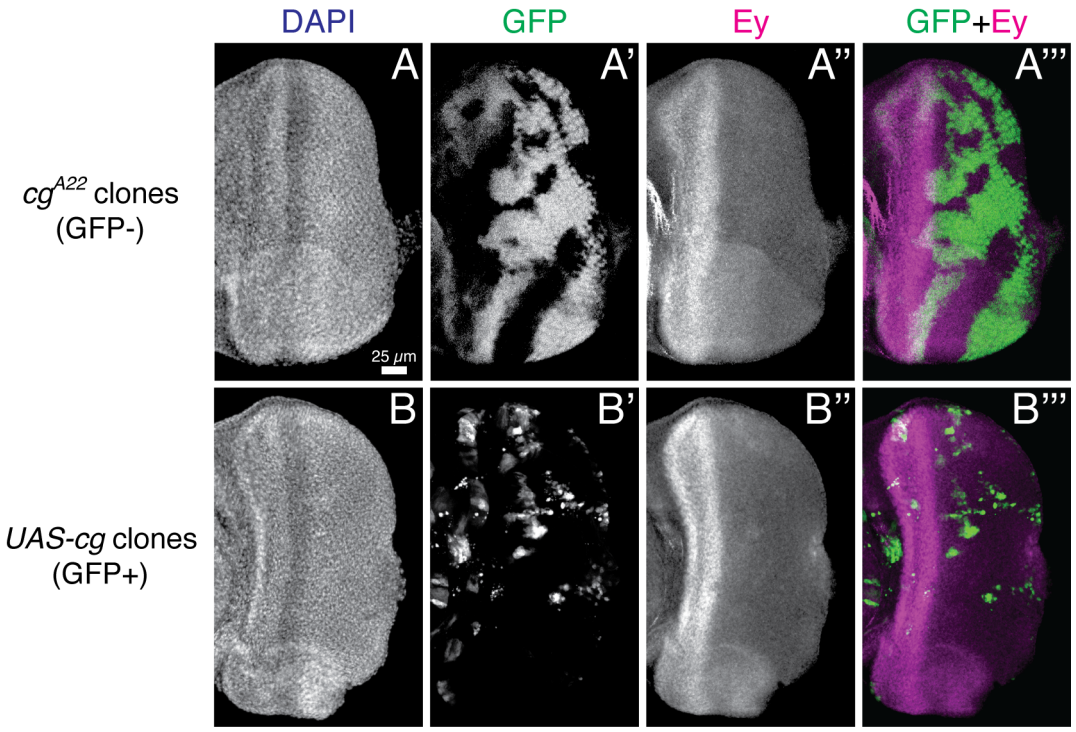

Fig. S8. *cg* does not control Ey expression in the eye imaginal disc. All images are maximum confocal projections of late third instar eye-antennal imaginal discs. Anterior is to the left and dorsal is up. (A) Mitotic *cg* clones do not affect Ey levels anterior to the MF or de-repress Ey posterior to the MF. (B) *FLP-out* clones overexpressing *cg* do not lower Ey levels in the preproneural domain or affect expression posterior to the MF.

Figure	Genotype	PH3+ Nuclei	MF length (μm)	PH3+ nuclei/μm MF	Normalization factor	Normalized
1G	*GMR-GAL4/+*	84	553.657	0.151718483	0.130309313	1.164295006
1G	*GMR-GAL4/+*	71	546.557	0.129904109	0.130309313	0.996890441
1G	*GMR-GAL4/+*	86	577.453	0.14892987	0.130309313	1.142895054
1G	*GMR-GAL4/+*	72	560.545	0.128446423	0.130309313	0.985704087
1G	*GMR-GAL4/+*	69	593.247	0.116309058	0.130309313	0.892561364
1G	*GMR-GAL4/+*	86	623.529	0.137924619	0.130309313	1.058440229
1G	*GMR-GAL4/+*	80	592.12	0.135107748	0.130309313	1.036823424
1G	*GMR-GAL4/+*	53	563.026	0.094134196	0.130309313	0.722390395
1G	*GMR-GAL4,UAS-eyaRNAi/+*	81	469.539	0.172509632	0.130309313	1.323847294
1G	*GMR-GAL4,UAS-eyaRNAi/+*	71	453.067	0.156709714	0.130309313	1.202597957
1G	*GMR-GAL4,UAS-eyaRNAi/+*	90	481.892	0.186763839	0.130309313	1.433234774
1G	*GMR-GAL4,UAS-eyaRNAi/+*	58	287.487	0.201748253	0.130309313	1.548225893
1G	*GMR-GAL4,UAS-eyaRNAi/+*	104	456.654	0.227743543	0.130309313	1.747715013
1G	*GMR-GAL4,UAS-eyaRNAi/+*	77	432.304	0.1781154	0.130309313	1.366866234
1G	*GMR-GAL4,UAS-eyaRNAi/+*	75	498.05	0.15058729	0.130309313	1.155614182
1G	*GMR-GAL4,UAS-eyaRNAi/+*	88	495.807	0.177488418	0.130309313	1.36205474
1G	*GMR-GAL4,UAS-eyaRNAi/+*	95	506.719	0.187480635	0.130309313	1.438735502
1G	*GMR-GAL4,UAS-eyaRNAi/+*	74	447.314	0.165431889	0.130309313	1.269532352
1G	*GMR-GAL4/UAS-soRNAi*	104	582.543	0.178527594	0.130309313	1.370029426
1G	*GMR-GAL4/UAS-soRNAi*	109	578.237	0.188504022	0.130309313	1.446589019
1G	*GMR-GAL4/UAS-soRNAi*	79	443.23	0.178237033	0.130309313	1.367799647
1G	*GMR-GAL4/UAS-soRNAi*	92	546.714	0.168278113	0.130309313	1.291374409
1G	*GMR-GAL4/UAS-soRNAi*	68	410.579	0.165619771	0.130309313	1.270974168
1G	*GMR-GAL4,UAS-eyaRNAi/UAS-soRNAi*	97	508.816	0.190638659	0.130309313	1.462970331
1G	*GMR-GAL4,UAS-eyaRNAi/UAS-soRNAi*	76	491.94	0.154490385	0.130309313	1.185566719
1G	*GMR-GAL4,UAS-eyaRNAi/UAS-soRNAi*	102	488.77	0.208687113	0.130309313	1.601475039
1G	*GMR-GAL4,UAS-eyaRNAi/UAS-soRNAi*	96	475.836	0.201750183	0.130309313	1.548240703
1G	*GMR-GAL4,UAS-eyaRNAi/UAS-soRNAi*	87	506.787	0.171669755	0.130309313	1.317402037
1G	*GMR-GAL4,UAS-eyaRNAi/UAS-soRNAi*	93	572.223	0.162524051	0.130309313	1.247217461
1G	*GMR-GAL4,UAS-eyaRNAi/UAS-soRNAi*	100	530.329	0.188562194	0.130309313	1.447035439
1G	*GMR-GAL4,UAS-eyaRNAi/UAS-soRNAi*	58	364.011	0.159335844	0.130309313	1.222751008
1G	*GMR-GAL4,UAS-eyaRNAi/UAS-soRNAi*	106	578.081	0.183365307	0.130309313	1.407154272
1G	*GMR-GAL4,UAS-eyaRNAi/UAS-soRNAi*	85	565.587	0.15028634	0.130309313	1.153304671
S2I	*GMR-GAL4/+*	56	546.87	0.102400936	0.102578397	0.99827
S2I	*GMR-GAL4/+*	56	507.89	0.110260096	0.102578397	1.074886127
S2I	*GMR-GAL4/+*	54	415.436	0.129983921	0.102578397	1.267166621
S2I	*GMR-GAL4/+*	50	473.211	0.105661111	0.102578397	1.030052274
S2I	*GMR-GAL4/+*	54	651.113	0.082934913	0.102578397	0.808502721
S2I	*GMR-GAL4/+*	58	576.345	0.100634169	0.102578397	0.981046418
S2I	*GMR-GAL4/+*	43	522.491	0.082298068	0.102578397	0.80229435
S2I	*GMR-GAL4/+*	56	526.049	0.106453962	0.102578397	1.03778149
S2I	*GMR-GAL4,UAS-eyaRNAi/+*	50	542.78	0.092118354	0.102578397	0.89802879
S2I	*GMR-GAL4,UAS-eyaRNAi/+*	57	305.253	0.186730352	0.102578397	1.820367224
S2I	*GMR-GAL4,UAS-eyaRNAi/+*	89	545.114	0.163268601	0.102578397	1.59164703
S2I	*GMR-GAL4,UAS-eyaRNAi/+*	81	502.32	0.161251792	0.102578397	1.571985882
S2I	*GMR-GAL4,UAS-eyaRNAi/+*	69	528.263	0.130616757	0.102578397	1.273335918
S2I	*GMR-GAL4,UAS-eyaRNAi/+*	100	504.654	0.198155568	0.102578397	1.931747561
S2I	*GMR-GAL4,UAS-eyaRNAi/+*	57	303.503	0.18780704	0.102578397	1.830863471
S2I	*GMR-GAL4,UAS-eyaRNAi/+*	87	435.5	0.199770379	0.102578397	1.947489773
S2I	*GMR-GAL4,UAS-eyaRNAi/+*	71	426.822	0.16634569	0.102578397	1.621644467
S2I	*GMR-GAL4,UAS-eyaRNAi/+*	87	466.761	0.186390894	0.102578397	1.817057972
S2I	*GMR-GAL4,UAS-eyaRNAi/UAS-stgRNAi*	62	535.699	0.115736636	0.102578397	1.128274951
S2I	*GMR-GAL4,UAS-eyaRNAi/UAS-stgRNAi*	60	470.661	0.127480288	0.102578397	1.242759609
S2I	*GMR-GAL4,UAS-eyaRNAi/UAS-stgRNAi*	50	436.585	0.114525236	0.102578397	1.116465446
S2I	*GMR-GAL4,UAS-eyaRNAi/UAS-stgRNAi*	64	461.825	0.138580631	0.102578397	1.35097287
S2I	*GMR-GAL4,UAS-eyaRNAi/UAS-stgRNAi*	50	496.471	0.100710817	0.102578397	0.981793633
S2I	*GMR-GAL4,UAS-eyaRNAi/UAS-stgRNAi*	57	580.011	0.098273998	0.102578397	0.958037962
S2I	*GMR-GAL4,UAS-eyaRNAi/UAS-stgRNAi*	44	408.776	0.107638413	0.102578397	1.049328284
S2I	*GMR-GAL4,UAS-eyaRNAi/UAS-stgRNAi*	82	611.203	0.134161645	0.102578397	1.30789376
S2I	*GMR-GAL4,UAS-eyaRNAi/pnt*	22	172.467	0.127560635	0.102578397	1.243542877
S2I	*GMR-GAL4,UAS-eyaRNAi/pnt*	63	445.858	0.141300593	0.102578397	1.377488806
S2I	*GMR-GAL4,UAS-eyaRNAi/pnt*	50	433.299	0.115393758	0.102578397	1.12493236
S2I	*GMR-GAL4,UAS-eyaRNAi/pnt*	42	350.635	0.11978268	0.102578397	1.167718386
S2I	*GMR-GAL4,UAS-eyaRNAi/pnt*	48	323.991	0.148152263	0.102578397	1.44428328
S2I	*GMR-GAL4,UAS-eyaRNAi/pnt*	49	376.237	0.130237058	0.102578397	1.269634367
S2I	*GMR-GAL4,UAS-eyaRNAi/pnt*	28	186.737	0.149943503	0.102578397	1.461745436
S2I	*GMR-GAL4,UAS-eyaRNAi/pnt*	46	417.809	0.110098155	0.102578397	1.073307424
S2I	*GMR-GAL4,UAS-eyaRNAi/pnt*	62	490.58	0.126381018	0.102578397	1.23204322
S2I	*GMR-GAL4,UAS-eyaRNAi/pnt*	39	366.191	0.106501798	0.102578397	1.038247833
S2I	*GMR-GAL4,UAS-eyaRNAi/ttk*	115	574.588	0.200143407	0.102578397	1.951126291
S2I	*GMR-GAL4,UAS-eyaRNAi/ttk*	105	504.722	0.208035314	0.102578397	2.028061661
S2I	*GMR-GAL4,UAS-eyaRNAi/ttk*	129	530.986	0.242944258	0.102578397	2.368376436
S2I	*GMR-GAL4,UAS-eyaRNAi/ttk*	122	542.435	0.224911741	0.102578397	2.192583895
S2I	*GMR-GAL4,UAS-eyaRNAi/ttk*	125	606.749	0.206015997	0.102578397	2.008376064
S2I	*GMR-GAL4,UAS-eyaRNAi/ttk*	92	492.543	0.186785722	0.102578397	1.820907011
4G	*GMR-GAL4/+*	56	546.87	0.102400936	0.102578397	0.99827
4G	*GMR-GAL4/+*	56	507.89	0.110260096	0.102578397	1.074886127
4G	*GMR-GAL4/+*	54	415.436	0.129983921	0.102578397	1.267166621
4G	*GMR-GAL4/+*	50	473.211	0.105661111	0.102578397	1.030052274
4G	*GMR-GAL4/+*	54	651.113	0.082934913	0.102578397	0.808502721
4G	*GMR-GAL4/+*	58	576.345	0.100634169	0.102578397	0.981046418
4G	*GMR-GAL4/+*	43	522.491	0.082298068	0.102578397	0.80229435
4G	*GMR-GAL4/+*	56	526.049	0.106453962	0.102578397	1.03778149
4G	*GMR-GAL4,UAS-eyaRNAi/+*	50	542.78	0.092118354	0.102578397	0.89802879
4G	*GMR-GAL4,UAS-eyaRNAi/+*	57	305.253	0.186730352	0.102578397	1.820367224
4G	*GMR-GAL4,UAS-eyaRNAi/+*	89	545.114	0.163268601	0.102578397	1.59164703
4G	*GMR-GAL4,UAS-eyaRNAi/+*	81	502.32	0.161251792	0.102578397	1.571985882
4G	*GMR-GAL4,UAS-eyaRNAi/+*	69	528.263	0.130616757	0.102578397	1.273335918
4G	*GMR-GAL4,UAS-eyaRNAi/+*	100	504.654	0.198155568	0.102578397	1.931747561
4G	*GMR-GAL4,UAS-eyaRNAi/+*	57	303.503	0.18780704	0.102578397	1.830863471
4G	*GMR-GAL4,UAS-eyaRNAi/+*	87	435.5	0.199770379	0.102578397	1.947489773
4G	*GMR-GAL4,UAS-eyaRNAi/+*	71	426.822	0.16634569	0.102578397	1.621644467
4G	*GMR-GAL4,UAS-eyaRNAi/+*	87	466.761	0.186390894	0.102578397	1.817057972
4G	*GMR-GAL4,UAS-eyaRNAi/cg*	56	495.476	0.113022629	0.102578397	1.101817071
4G	*GMR-GAL4,UAS-eyaRNAi/cg*	53	466.863	0.113523668	0.102578397	1.106701518
4G	*GMR-GAL4,UAS-eyaRNAi/cg*	64	460.657	0.138932004	0.102578397	1.354398274
4G	*GMR-GAL4,UAS-eyaRNAi/cg*	58	536.181	0.108172427	0.102578397	1.054534192
4G	*GMR-GAL4,UAS-eyaRNAi/cg*	63	611.002	0.103109319	0.102578397	1.005175767
4G	*GMR-GAL4/cg*	68	652.935	0.104145129	0.102578397	1.015273512
4G	*GMR-GAL4/cg*	57	554.549	0.102786228	0.102578397	1.002026072
4G	*GMR-GAL4/cg*	57	536.036	0.106336142	0.102578397	1.036632906
4G	*GMR-GAL4/cg*	49	520.675	0.094108609	0.102578397	0.917431076
4G	*GMR-GAL4/cg*	62	520.633	0.119085805	0.102578397	1.160924803
4G	*GMR-GAL4/cg*	55	403.476	0.136315419	0.102578397	1.328890129

Figure	Genotype	PH3+ Nuclei	MF length (μm)	PH3+ nuclei/μm MF	Normalization factor	Normalized
4K	*w1118*	30	474.36	0.063243107	0.073939409	0.855336925
4K	*w1118*	34	442.618	0.076815674	0.073939409	1.038900301
4K	*w1118*	37	517.855	0.071448572	0.073939409	0.966312454
4K	*w1118*	35	523.093	0.066909708	0.073939409	0.9049262
4K	*w1118*	46	503.944	0.091279983	0.073939409	1.23452412
4K	*cg*	29	488.364	0.059381936	0.073939409	0.803116192
4K	*cg*	35	523.413	0.066868802	0.073939409	0.904372954
4K	*cg*	29	524.637	0.055276315	0.073939409	0.747589355
4K	*cg*	50	420.637	0.118867337	0.073939409	1.607631694
4K	*cg*	37	433.189	0.085413065	0.073939409	1.155176461
4K	*w1118*	25	486.592	0.051377746	0.079716795	0.6445034
4K	*w1118*	41	425.862	0.096275319	0.079716795	1.207716879
4K	*w1118*	43	505.89	0.084998715	0.079716795	1.066258557
4K	*w1118*	38	556.629	0.068268092	0.079716795	0.8563828
4K	*w1118*	45	491.34	0.091586274	0.079716795	1.148895586
4K	*w1118*	25	286.856	0.087151742	0.079716795	1.093267
4K	*w1118*	21	348.586	0.060243383	0.079716795	0.755717575
4K	*w1118*	37	583.373	0.063424259	0.079716795	0.795619773
4K	*w1118*	45	497.627	0.090429177	0.079716795	1.134380484
4K	*w1118*	38	536.913	0.070774967	0.079716795	0.887830061
4K	*w1118*	48	559.981	0.085717194	0.079716795	1.075271448
4K	*w1118*	56	563.387	0.099398815	0.079716795	1.24689928
4K	*w1118*	55	577.684	0.095207761	0.079716795	1.194324988
4K	*w1118*	22	312.874	0.070315846	0.079716795	0.882070657
4K	*w1118*	29	359.879	0.08058264	0.079716795	1.010861512
4K	*cg*	7	318.452	0.021981335	0.079716795	0.27574283
4K	*cg*	4	305.762	0.01308207	0.079716795	0.164106827
4K	*cg*	19	341.995	0.055556368	0.079716795	0.696921741
4K	*cg*	19	323.141	0.058797862	0.079716795	0.73758437
4K	*cg*	24	345.843	0.069395651	0.079716795	0.870527351
4K	*cg*	6	497.179	0.012068088	0.079716795	0.151387021
4K	*cg*	14	295.148	0.04743383	0.079716795	0.595029311
4K	*cg*	9	447.52	0.020110833	0.079716795	0.252278494
4K	*cg*	19	454.301	0.041822492	0.079716795	0.524638402
4K	*cg*	16	389.32	0.041097298	0.079716795	0.515541269
4K	*cg*	14	327.433	0.042756839	0.079716795	0.536359228
4P	*w1118*	69	474.36	0.145459145	0.118448256	1.228039565
4P	*w1118*	68	442.618	0.153631348	0.118448256	1.297033431
4P	*w1118*	57	517.855	0.110069421	0.118448256	0.929261642
4P	*w1118*	61	523.093	0.116614063	0.118448256	0.984514814
4P	*w1118*	41	503.944	0.081358246	0.118448256	0.686867404
4P	*w1118*	54	407.467	0.13252607	0.118448256	1.118852011
4P	*w1118*	42	574.301	0.073132382	0.118448256	0.617420502
4P	*w1118*	69	511.887	0.134795375	0.118448256	1.138010631
4P	*cg*	20	515.697	0.038782463	0.118448256	0.32742114
4P	*cg*	18	488.364	0.036857754	0.118448256	0.311171774
4P	*cg*	40	523.413	0.076421487	0.118448256	0.645188789
4P	*cg*	39	524.637	0.074337113	0.118448256	0.627591451
4P	*cg*	22	420.637	0.052301628	0.118448256	0.441556758
4P	*cg*	26	460.123	0.05650663	0.118448256	0.477057509
4P	*cg*	26	433.189	0.060019991	0.118448256	0.506719077
4P	*cg*	31	454.528	0.068202619	0.118448256	0.575800955
4P	*cg*	16	514.268	0.031112183	0.118448256	0.262664762
4P	*cg,eya/cg*	16	182.531	0.087656343	0.079716795	1.099596929
4P	*cg,eya/cg*	16	207.106	0.077255125	0.079716795	0.969119808
4P	*cg,eya/cg*	24	293.887	0.081664041	0.079716795	1.024427043
4P	*cg,eya/cg*	31	371.614	0.083419893	0.079716795	1.046453164
4P	*cg,eya/cg*	19	346.394	0.054850835	0.079716795	0.688071245
4P	*cg,eya/cg*	22	264.687	0.08311704	0.079716795	1.042654058
4P	*cg,eya/cg*	19	268.543	0.07075217	0.079716795	0.887544083
4P	*cg,eya/cg*	32	322.333	0.099276214	0.079716795	1.245361331
4P	*cg,eya/cg*	35	372.252	0.094022329	0.079716795	1.17945445
4P	*cg,eya/cg*	30	295.35	0.101574403	0.079716795	1.27419075
4P	*cg,eya/cg*	34	340.11	0.099967658	0.079716795	1.254035077
4P	*cg,eya/cg*	34	360.751	0.094247833	0.079716795	1.182283264
4P	*cg,eya/cg*	41	495.548	0.082736687	0.079716795	1.037882759
4P	*cg,eya/cg*	31	414.68	0.074756439	0.079716795	0.937775263
4P	*cg,so/cg*	37	517.049	0.071559949	0.118448256	0.604145229
4P	*cg,so/cg*	34	423.706	0.08024432	0.118448256	0.677463079
4P	*cg,so/cg*	39	290.777	0.1341234	0.118448256	1.132337485
4P	*cg,so/cg*	36	391.558	0.091940402	0.118448256	0.776207309
4P	*cg,so/cg*	29	418.977	0.06921621	0.118448256	0.584358202
4P	*cg,so/cg*	35	433.791	0.080684016	0.118448256	0.681175212
4P	*cg,so/cg*	31	266.749	0.116214119	0.118448256	0.981138285
4P	*cg,so/cg*	42	386.117	0.108775319	0.118448256	0.918336183
4P	*cg,so/cg*	41	381.308	0.107524626	0.118448256	0.907777195

Table S1. Raw counts of PH3$^+$ nuclei, measurements of MF length, and normalizations used to quantify the fraction of mitotic cells at the SMW. All PH3$^+$ nuclei in the SMW were manually counted using the multi-point selection tool in FIJI and divided by the length of the MF, measured with the segmented line tool, to obtain the number of mitotic cells per micron of the MF. Counts and measurements were carried out in unaltered confocal images to retain the three-dimensional nature of the tissue, and measurements included the entire length of the SMW,

including in cases where parts of the tissue folded under the rest of the disc. In rare instances where $PH3^{+}$ nuclei could not be resolved unambiguously, that portion of the disc was not analyzed. Figs. 1X and 4G present data for *GMR/+* and eya^{RNAi} from the same experiment that was carried out in parallel. Fig. 1G has the same sample sizes, but represents data from a different experiment.